Theoretical Study of Cation/Ether Complexes: The Alkali Metals and Dimethyl Ether

Susan E. Hill,* Eric D. Glendening,† and David Feller

Environmental Molecular Sciences Laboratory, Pacific Northwest National Laboratory, 906 Battelle Boulevard, MS K1-90, Richland, Washington 99352

Received: March 31, 1997; In Final Form: June 5, 1997[⊗]

The structures and binding enthalpies of a single alkali metal cation complexed with up through four dimethyl ether (DME) ligands were obtained with Hartree−Fock wave functions and second-order perturbation theory, with consideration of core/valence correlation and relativistic effects. The basis sets used in this study included diffuse functions on oxygen, in order to minimize undesirable basis set superposition error, and polarization functions on all non-hydrogen atoms. The observed trends in complex formation energy along the sequence of cations are discussed and compared to the available experimental data obtained from collision-induced dissociation measurements. Minimum energy $M^+(DME)_2$ geometries are predicted to be linear for the light metal complexes and bent for the heavy metal complexes.

I. Introduction

Complexes comprised of a single metal cation and one or more neutral ligands have recently been the focus of a number of theoretical[1−7] and experimental studies.[8−11] As is often the case when theory and experiment simultaneously probe the same chemical systems, those systems act as a synergistic interface between the two approaches. In ideal situations, opportunities are created for each approach to exploit the strengths of the other, thereby advancing faster than it could on its own. In the case of cation/ligand complexes, typically dominated by strong electrostatic forces, *ab initio* theory brings to bear its expertise in determining accurate molecular structures, vibrational frequencies, and, when performed at sufficiently high levels, accurate binding energies. However, for moderate-to-large chemical systems, reliable experimental values are important for calibrating the computational models. Two examples of the complementary roles of theory and experiment in this area of research have appeared in recent works by More et al.[9] on Li^+: dimethyl ether (DME) complexes and Ray et al.[10] on Li^+: dimethoxyethane and Li^+:12-crown-4 complexes.

Although computational studies of cation−ligand complexes first appeared in the chemical literature as early as 1972,[12] reports of complexes with more than a dozen atoms are still rare. Several studies have focused on the $M^+(H_2O)_n$ clusters, which serve as solvation models for alkali,[13−16] alkaline earth,[17−19] transition metal,[20−23] and rare earth[17] cations. In these cases, a comparison of ligand binding affinities for metal cations with different charges and polarizabilities has been instrumental in distinguishing quantum mechanical structural influences from mainly electrostatic ones. This analysis is expected to be particularly important in predicting whether cation/biligand complexes and MX_2 molecules[24−26] are linear or bent, and whether incremental ligand binding energies decrease monotonically with increasing coordination.[21]

Bauschlicher et al. [13] studied $Na^+(H_2O)_x$, $x = 1-4$, with second-order Møller−Plesset perturbation theory (MP2) and higher levels of theory, finding the successive ligand binding energies to be rather insensitive to electron correlation and to decrease monotonically with increasing ligand number. The water molecules of the $Na^+(H_2O)_2$ system were found to coordinate the metal in a linear fashion, as expected from a simple electrostatic model of a cation interacting with two polar ligands. Glendening and Feller[16] also studied alkali cation/water clusters (Li^+ through Cs^+), finding the heavy metal/$(H_2O)_2$ complexes to favor nonclassical bent structures. This observation was explained in terms of metal core polarization by the ligands, consistent with the metal size dependence in the linear-to-bent trend. The same mechanism is responsible for other nonclassical symmetry lowering, such as pyramidal distortions of planar metal/triligand clusters.

Core polarization has also been observed for the alkaline earth/water complexes.[17−19] In particular, Bauschlicher and coworkers[18] found a bent structure for the more polarizable Mg^+ with two waters, whereas $Mg^{2+}(H_2O)_2$ was shown to be linear.[19] In the alkaline earth systems, there is also a small covalent contribution from the low-lying d orbitals which favors bent structures.[17,18] Participation of d orbitals is especially important in determining metal−ligand structures for rare earth[27] and transition metal[20−22,28] complexes, and it is likely to produce a deviation from purely monotonic trends in incremental energies.

Ligand polarization also contributes to deviations from classical bonding behavior. A combined theoretical/experimental study of Li^+ complexed with DME, CH_3OCH_3, by More et al.[9] revealed that, despite its smaller dipole moment, DME binds more strongly to Li^+ than does water.[14,29] This was attributed to the polarizability of DME, which is nearly 4 times larger than that of water.

In this paper we examine complexes composed of a single alkali metal cation (Li^+-Cs^+) and up through four DME ligands using restricted Hartree−Fock geometries with MP2 energy corrections. Calculations of these complexes are performed at the restricted Hartree−Fock (RHF) and second-order Møller−Plesset (MP2) perturbation levels of theory with polarized basis sets. These simple metal/ether systems are intended to model the basic interactions found in cation/crown ether[30] adducts (rather than acting as solvation models). Complexes with four DME ligands represent the acyclic analogs of the M^+:12-crown-4 systems, but without the internal constraints imposed by the crown ether macrocycle. Crown ethers have received considerable attention recently as potential molecular sequestering agents for cations in waste solution.[31−33] The present work is part of an ongoing research project involving studies of mono- and divalent cations interacting with larger polyether molecules, as well as crowns themselves.

† Current address: Department of Chemistry, Indiana State University, Terre Haute, IN 47809.

⊗ Abstract published in *Advance ACS Abstracts,* August 1, 1997.

S1089-5639(97)01124-9 CCC: $14.00

TABLE 1: MP2 Incremental Binding Energies Computed with Different Counterpoise Definitions[a]

	$Li^+(DME)_x$	
x	ΔE_i(CP:A)	ΔE_i(CP:B)
2	−33.0	−32.6
3	−24.6	−23.7
4	−16.7	−16.3

[a] Binding energies are in kcal/mol. All calculations were done with the 6-31+G* basis set at RHF optimized geometries. Definitions "A" and "B" are defined in the text.

II. Procedure

Incremental $Li^+(DME)_x$, $x = 1-4$, binding enthalpies at 298 K were recently reported by More et al.[9] as part of their ongoing experimental/theoretical investigation of cation/ligand complexes. The experimental portion of the work involved the analysis of thresholds for collision-induced dissociation (CID) with xenon. The theoretical portion consisted of the evaluation of optimal geometries, binding energies and enthalpies, and vibrational frequencies at the RHF and MP2 levels of theory. The experimental and calculated MP2 binding enthalpies differed by less than 2 kcal/mol per metal−oxygen interaction. The counterpoise correction (CP) of Boys and Bernardi[34] was applied to the calculated values to account for the undesirable effects of basis set superposition error (BSSE). The CP correction was computed using the so-called "relaxed fragment" geometries. The same level of theory provided exceptionally good agreement with the complete basis set limit estimated from much larger correlation consistent basis sets[35] for the binding energy of the Li^+(DME) complex.

Two of the quantities of interest in these systems are the total and the incremental binding energies. The former is defined as ΔE for the reaction

$$M^+ + x\text{DME} \rightarrow M^+(\text{DME})_x, \quad x = 1-4 \tag{1}$$

while the latter corresponds to ΔE for the reaction

$$M^+(\text{DME})_{x-1} + \text{DME} \rightarrow M^+(\text{DME})_x \tag{2}$$

Since there has been discussion in the literature[36−38] over how the CP correction should be applied in the case of multiple ligands, we now discuss the approach we chose to use. The primary issues with molecular aggregates concern additivity and the order in which CP corrections are applied. The counterpoise correction for the total binding energy for an $M^+(DME)_x$ complex consists of $2x+1$ component calculations. The metal cation and the ligands are each computed separately in the cluster geometry in the presence of the full "ghost" cluster basis functions and, in the case of the ligands, at their cluster geometry without the ghost functions. One recognizes, however, that CP-adjusted incremental binding energies could be computed as (A) the difference between the two CP-corrected total binding energies for $M^+(DME)_{x-1}$ and $M^+(DME)_x$ using eq 1 or (B) the raw binding energy of eq 2 minus the CP correction computed for $M^+(DME)_{x-1}$ and DME fragments. In the complete basis set limit the two definitions should be identical. Complete basis set estimates on complexes the size of $M^+(DME)_2$, the smallest relevant complex that might be used to distinguish between the two CP approaches, remain prohibitively expensive computationally.

The BSSE ranges for $Li^+(DME)_x$ and $Cs^+(DME)_x$ are 1.8−4.9 kcal/mol and 1.5−1.7 kcal/mol, respectively, for $x = 1-4$. This is for an MP2 correction at the RHF geometry using method B. Table 1 compares MP2 incremental binding energies obtained from both approaches for $Li^+(DME)_x$. Since the magnitude of the CP correction is larger for these more strongly bound adducts, the incremental binding energies for these complexes should depend more strongly on the CP approach selected than the energies of the complexes involving heavier cations. In the worst case, the difference in binding energies calculated by methods A and B amounts to 0.9 kcal/mol, or approximately 4% of the value. For Cs^+, which has longer metal−oxygen distances and less BSSE, the maximum difference is 0.2 kcal/mol. Thus, for all but the most demanding of studies, the uncertainty introduced by the choice of counterpoise methods is negligible for these electrostatic aggregates. In the present study we shall report incremental binding energies computed with method A for the sake of consistency with our previous work.

Unless otherwise noted, all $M^+(DME)_x$ calculations in this work were performed with the diffuse function-augmented 6-31+G* basis sets[39−41] on H, Li, O, and Na. The somewhat smaller 6-31G* basis set was used on C, following the example set in the earlier work.[5,16,19] The presence of the diffuse (sp) functions on oxygen is important in reducing BSSE, whereas their presence on carbon was demonstrated to have relatively little impact on either energetics or structure.[3]

Effective core potentials (ECPs) by Hay and Wadt[42] were used for the heavier metals (K, Rb, and Cs), including valence functions for the $(n-1)s^2$ $(n-1)p^6$ shell. The valence basis sets are (5s5p)/[3s3p] contractions of Hay and Wadt's functions, augmented by six-term d-type polarization functions, energy-optimized by Glendening and co-workers[3] for the $M^+(H_2O)$ systems. For Rb and Cs the ECP includes the dominant relativistic effects (i.e. mass−velocity and Darwin corrections) on the valence electrons. The 6-31+G*/6-31G* hybrid basis and metal ECP basis together will be referred to as the 6-31+G* basis set in this paper. All calculations were performed with the Gaussian 92[43] and Gaussian 94[44] programs. Geometry optimizations used the "tight" convergence criterion, which corresponds to a maximum component of the force of $\leq 1.5 \times 10^{-5}$ E_h/bohr.

The Li, C, and O $1s^2$ inner shell electrons were treated as frozen cores (FCs) in the MP2 calculations. For Na^+-Cs^+ the electrons in the $(n-1)$ metal shell, e.g. the (2s,2p) shell in Na, were included in the correlation treatment. It has been shown that neglecting this shell results in an overestimation of the $M^+\cdots O$ bond length with a corresponding decrease in bond strength.[3] The impact of using different core definitions will be discussed for some of the $Na^+(DME)_x$ complexes.

Room-temperature (298 K) enthalpy corrections are computed using standard gas-phase expressions.[45] Harmonic frequencies for structures optimized at the RHF level have a 0.9 scaling factor applied. MP2 frequencies are unscaled. For a comparison of empirical scaling factors for frequencies calculated at various levels of theory, see the recent article by Scott and Radom.[46]

III. Results

A. M^+(DME). RHF and MP2 optimized structural parameters for the minimum energy configurations M^+(DME), M = Li, Na, K, Rb, Cs, series are shown in Figure 1, with the MP2 values given in parentheses. The Li^+(DME) parameters were taken from More et al.[9] All five complexes possess C_{2v} symmetry, with the $M^+\cdots O$ bond lying in the same plane as the heavy atom framework of the ether. As the ionic radius increases along the sequence Li^+-Cs^+, Pauli repulsion produces a corresponding increase in the metal−oxygen distance. As the distance separating the positively charged metal and the ether

TABLE 2: RHF and MP2 Total Binding Energies and Enthalpies for $M^+(DME)_x$ Obtained with the 6-31+G* Hybrid Basis Set[a]

	total binding energy ΔE_t					total binding enthalpy ΔH_t^{298}				
x	Li[b]	Na	K	Rb	Cs	Li[b]	Na	K	Rb	Cs
					RHF @ RHF Geometry					
1	−39.6	−26.6	−18.4	−15.3	−13.0	−38.8	−26.1	−17.9	−14.8	−12.5
2	−72.3	−49.7	−34.3	−28.8	−24.4	−69.9	−47.7	−32.5	−26.9	−22.7
3	−95.0	−68.0	−48.2	−40.7	−34.5	−91.0	−64.7	−45.1	−37.6	−31.5
4	−107.9	−81.6	−59.7	−50.8	−43.4	−102.5	−76.9	−56.5	−46.5	−39.0
					MP2 @ RHF Geometry					
1	−39.1	−26.8	−19.5	−16.4	−14.1	−38.3	−26.2	−19.0	−15.9	−13.7
2	−72.1	−50.2	−36.6	−30.9	−26.8	−69.7	−48.2	−34.7	−29.1	−25.1
3	−96.7	−69.5	−51.8	−43.9	−38.0	−92.8	−66.2	−48.6	−40.8	−34.9
4	−113.4	−85.1	−64.9	−55.4	−48.1	−108.1	−80.5	−61.7	−51.1	−43.8
					MP2 @ MP2 Geometry					
1	−39.0	−26.5	−19.3	−16.2	−14.0	−38.2	−25.9	−18.8	−15.8	−13.6
2	−71.7	−49.8	−36.1	−30.5	−26.4	−69.3	−47.8	−34.2	−28.6	−24.6

[a] Counterpoise-corrected binding energies and enthalpies (298 K) are given in kcal/mol. [b] More et al.[9]

TABLE 3: Incremental Binding Energies and Enthalpies for $M^+(DME)_x$ Obtained with the 6-31+G* Hybrid Basis Set[a]

	incremental binding energy ΔE_i					incremental binding enthalpy ΔH_i^{298}				
x	Li[b]	Na	K	Rb	Cs	Li[b]	Na	K	Rb	Cs
					RHF @ RHF Geometry					
1	−39.6	−26.6	−18.4	−15.3	−13.0	−38.8	−26.1	−17.9	−14.8	−12.5
2	−32.7	−23.1	−15.9	−13.5	−11.4	−31.1	−21.6	−14.6	−12.1	−10.2
3	−22.7	−18.3	−13.9	−11.9	−10.1	−21.1	−17.0	−12.6	−10.7	−8.8
4	−12.9	−13.6	−11.5	−10.1	−8.9	−11.5	−12.2	−11.4	−8.9	−7.5
					MP2 @ RHF Geometry					
1	−39.1	−26.8	−19.5	−16.4	−14.1	−38.3	−26.2	−19.0	−15.9	−13.7
2	−33.0	−23.4	−17.1	−14.5	−12.7	−31.4	−22.0	−15.7	−13.2	−11.4
3	−24.6	−19.3	−15.2	−13.0	−11.2	−23.1	−18.0	−13.9	−11.7	−9.8
4	−16.7	−15.6	−13.1	−11.5	−10.1	−15.3	−14.3	−13.1	−10.3	−8.9
					MP2 @ MP2 Geometry					
1	−39.0	−26.5	−19.3	−16.2	−14.0	−38.2	−25.9	−18.8	−15.8	−13.6
2	−32.7	−23.3	−16.8	−14.3	−12.4	−31.1	−21.9	−15.4	−12.8	−11.0

[a] Counterpoise-corrected binding energies and enthalpies (298 K) are given in kcal/mol. [b] More et al.[9]

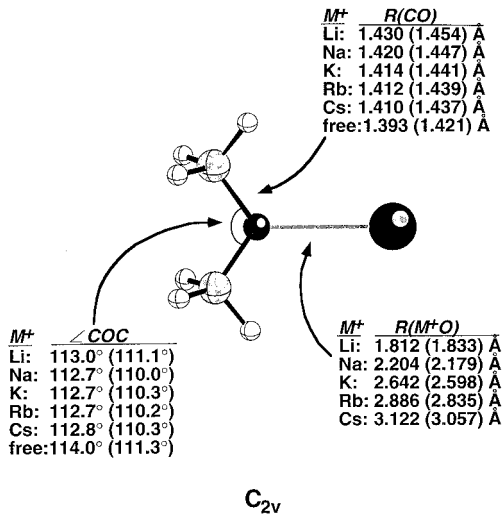

Figure 1. $M^+(DME)$ C_{2v}, RHF and MP2/6-31+G* optimized structures. MP2 parameters are given in parentheses. The Li data were taken from ref 9.

oxygen (which bears a partial negative charge) increases, the strength of this predominantly electrostatic bond decreases. Correlation recovery at the MP2 level shortens most of the metal−oxygen bond lengths, with the greatest effect (−0.07 Å) observed for Cs^+, which is the most polarizable of the metals. The magnitude of the correlation correction gradually diminishes with decreasing cation size. For Li^+, there is an increase due to neglect of the $1s^2$ shell. Correlating the $1s^2$ electrons would shorten the $Li^+\cdots O$ bond length from 1.833 to 1.789 Å, although the metal/ether binding energy changes by less than 0.1 kcal/mol. The C−O bond length smoothly approaches the free DME value as the metal−oxygen distance increases. The C−O−C angle is insensitive to the metal in these systems.

According to Hay and Rustad,[47] a simple aliphatic ether/metal system like the $M^+(DME)$ configuration could establish the "ideal" structural criteria for predicting optimal metal/crown ether binding. It is generally understood that optimizing the $M^+\cdots O$ bond length in a metal/crown complex (i.e. fitting the cation in the crown cavity) will lead to enhanced selection of the cation by that crown. By applying *ab initio* and molecular mechanics techniques to some metal/ether complexes, Hay and Rustad were able to put forward another important criterion for favorable binding: the orientation of the donor oxygen. For the metal/ether complexes, a trigonal planar arrangement of the cation with the C−O−C moiety is preferred. Satisfying this orientational criterion appears to be at least as important as optimizing the $M^+\cdots O$ bond length.[47,48] All of the DME ligands in this work exhibited a C−O−C dipole directed towards the cation.

The total binding energies (ΔE_t) and corresponding enthalpies at 298 K (ΔH_t^{298}) are given in Table 2. Incremental binding energies (ΔE_i) are provided in Table 3. Since one of the goals of the present study was to benchmark the accuracy of the methods we use for treating large crown ether complexes, we examined the consequences of substituting RHF geometries in place of MP2 geometries when computing binding energies. In three previous studies[6,9,10] that examined the same issue in different complexes, the magnitude of the effect was less than

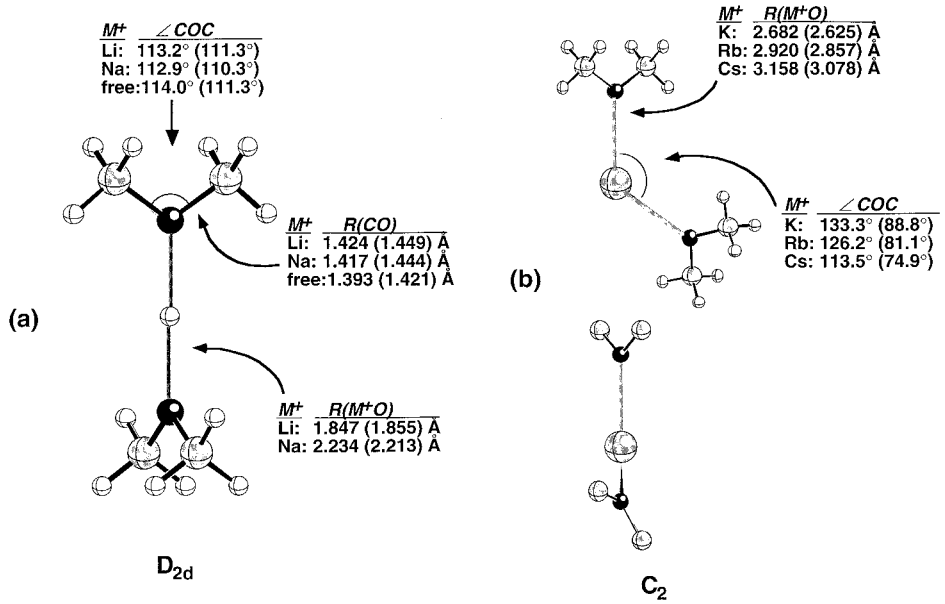

Figure 2. $M^+(DME)_2$ RHF and MP2/6-31+G* optimized structures. (a) Linear D_{2d} structures for M = Li, Na. (b) Bent C_2 structures for M = K, Rb, Cs. Views show the C−O−C plane parallel to the paper, and normal to the paper with hydrogens not shown. The Li data were taken from ref 9.

1 kcal/mol. Although the binding energy of the first ligand drops by a factor of 3 from Li^+ to Cs^+, the MP2 corrected binding energies at RHF or MP2 geometries vary by less than 0.2 kcal/mol. This provides further justification for the use of RHF geometries in larger cation/ether clusters, although certain consequences of the approximation will be pursued later.

Calculations of the binding energy performed with larger basis sets suggest that the errors attributable to basis truncation with the 6-31+G* basis should be on the order of ±2 kcal/mol or less. For example, the estimated complete basis set MP2 limit for ΔE in K^+(DME) was −19.7 kcal/mol,[6] compared to −19.5 kcal/mol (6-31+G*). The same comparison for Li^+(DME) yielded −38.5 kcal/mol (CBS limit) vs −39.1 kcal/mol (6-31+G*).[9]

B. $M^+(DME)_2$. RHF and MP2 geometry optimizations predict D_{2d} symmetry complexes for $Li^+(DME)_2$ and $Na^+(DME)_2$ (Figure 2a), whereas the heavier alkali metal cations produced bent structures with C_2 symmetry (Figure 2b). The collinear O−M$^+$−O alignment in the former complexes is in accord with a simple point charge−dipole model. The nonclassical structures adopted by $K^+(DME)_2$, $Rb^+(DME)_2$, and $Cs^+(DME)_2$ are probably the result of metal core polarization.[17] Bauschlicher et al., demonstrated the importance of core polarization to bending in $Sr^{2+}(H_2O)_2$ complexes by freezing the 4s and 4p orbitals for the bent geometry from the linear structure.[18] A bent conformation was predicted only when the core orbitals were allowed to relax. In a related 6-31+G* study of $M^+(H_2O)_n$ clusters, Glendening et al.[16] likewise reported bent structures for $M^+(H_2O)_2$, M = K, Rb, and Cs, although they noted that the energy differences between the "linear" D_{2d} structures and the bent structures were very small. In fact, with much larger basis sets and all-electron (AE) calculations, the linear form of $K^+(H_2O)_2$ was found to be 2.2 kcal/mol lower than the bent form at the MP2 level (using MP2 optimized geometries).[15]

As the size of the cation increases, the tendency to favor a highly bent structure increases, as can be seen for the five RHF bending potentials shown in Figure 3. The energies plotted in Figure 3 correspond to geometries in which the OM$^+$O angle was held fixed and all other internal coordinates were optimized. The bending potentials for the heavier metals show a significant

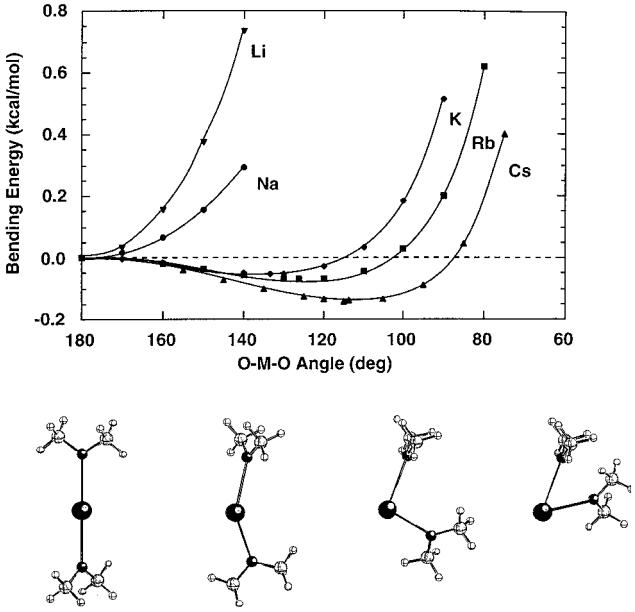

Figure 3. O−M−O bending potentials for the $M^+(DME)_2$ structures. Each calculated point represents the energy of an otherwise RHF/6-31+G* optimized structure, relative to the energy in the linear D_{2d} configuration.

anharmonic component. At the MP2 level of theory the depth of the K^+, Rb^+, and Cs^+ minima increase and are shifted by ∼30° relative to the RHF values (see Figure 4).

To determine the degree to which the use of ECPs and valence basis sets influence the calculated geometries, we reoptimized the $K^+(DME)_2$ complex with the aug-cc-pVDZ correlation consistent basis set.[35,49] The potassium ECP was replaced with an all-electron (15s,12p,2d) → [6s,5p,2d] contracted basis set[15] using Gaussian primitives reported by Schäfer and co-workers.[50] This basis set included an additional tight (s, p, d) shell. Not unexpectedly, at the RHF level a linear structure was predicted with a very shallow bending curve. At the MP2 level the predicted OK$^+$O angle (81.7°) differed very little from the MP2(ECP)/6-31+G* value (88.8°) despite the large increase in the number of basis functions relative to the 6-31+G*(ECP) basis set (137 → 277). The MP2/aug-cc-pVDZ

TABLE 4: Linearization Energies for $M^+(DME)_2$ Obtained with the 6-31+G* Basis Set[a]

method	geometry	K^+	Rb^+	Cs^+
RHF	RHF	0.05	0.07	0.14
MP2	RHF	0.33	0.39	0.52
MP2	MP2	0.90[b]	1.06	1.21

[a] Energies are given in kcal/mol. [b] The linearization energy at the MP2/aug-cc-pVDZ level is 1.3 kcal/mol.

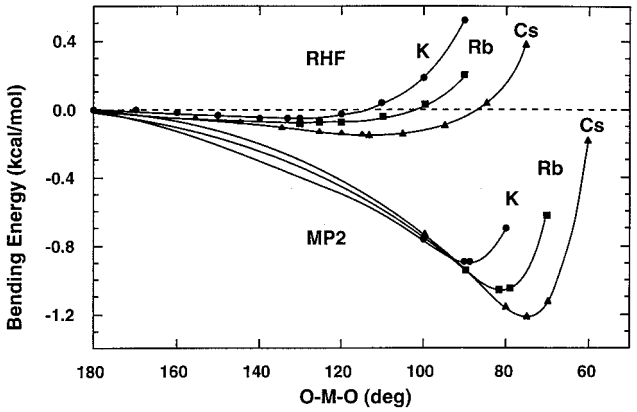

Figure 4. O−M−O bending potentials for the $M^+(DME)_2$ (M = K, Rb, Cs) structures otherwise optimized at both the RHF and MP2/6-31+G* levels of theory.

KO bond lengths were within 0.006 Å of the smaller basis set value. These findings suggest that MP2(ECP)/6-31+G* geometries should compare favorably with results obtained with much larger basis sets.

Table 4 lists RHF and MP2 linearization energies at the RHF and MP2 optimized geometries. Due to the flatness of RHF bending potentials, numerical precision became a problem when determining the harmonic frequencies of $Rb^+(DME)_2$ and $Cs^+(DME)_2$. Because Gaussian 92 and 94 do not provide analytical second derivatives for ECPs, finite difference methods were required. As a consequence of the inherent numerical noise, the lowest RHF harmonic frequency was 6i cm^{-1} for $Rb^+(DME)_2$ and 3i cm^{-1} for $Cs^+(DME)_2$. Similar small imaginary frequencies have been observed for large cation/water clusters when ECPs were used.[15] Such frequencies are below the level of accuracy ($\sim$10 cm^{-1}) for RHF calculations and have no physical significance. For an MP2 optimization, the frequencies corresponding to the RHF imaginary ones take on the real values of 20 (Rb) and 21 cm^{-1} (Cs), respectively.

The importance of d functions on metal/ligand complexes was emphasized in the work of Kaupp and Schleyer[17] with NH_3, H_2O, and HF ligands. They showed that a consequence of insufficient d functions is the prediction of artificially long metal−ligand distances for many clusters.[17,25] We observed similar behavior in $K^+(DME)_2$ when the potassium d function was removed. The $M^+\cdots O$ distance increased substantially, from 2.63 to 2.71 Å. All other structural changes were small. The effect of the d function on bending is probably more important for MX_2 molecules[26] or for Group II−III metal/ligand complexes, which exhibit somewhat greater covalent bonding character.

C. $M^+(DME)_3$. All of the $M^+(DME)_3$ complexes display D_3 symmetry. The metal cation and the three ether oxygens are coplanar. Optimized RHF/6-31+G* structural parameters for each of the alkali cations are shown in Figure 5. MP2 geometry optimizations and numerical frequency calculations were considered prohibitively expensive to do for each of the 20 complexes discussed here. The COM^+O torsion angle, which measures the methyl carbon tilt relative to the plane of

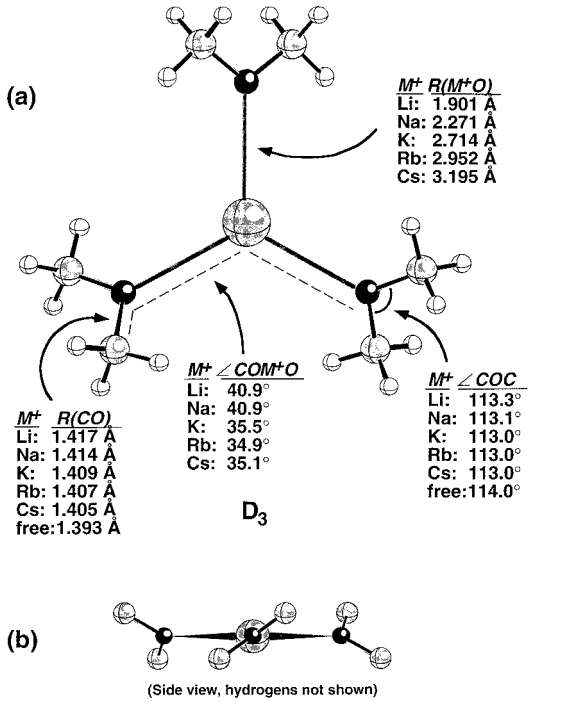

Figure 5. $M^+(DME)_3$ planar D_3, RHF/6-31+G* optimized structures. (a) O-plane parallel to the paper. (b) O-plane normal to the paper, with hydrogens absent. The Li data were taken from ref 9.

the ether oxygens, increases along with ligand−ligand repulsion as the $M^+\cdots O$ distance shrinks. Normal mode analyses yield small frequency motions, corresponding to a C_3 pyramidal distortion that are on the order of 10 cm^{-1}. $Cs^+(DME)_3$ was characterized by one imaginary frequency (3i cm^{-1}).

A "nonplanar" C_3 symmetry configuration of $Cs^+(DME)_3$ was also explored. Cesium was chosen because it was expected to exhibit the most pronounced structural deviation from planarity among the five cations. At the RHF level, the C_3 configuration was only 0.004 kcal/mol lower in energy than the planar (D_3) conformation. This value increased slightly to 0.2 kcal/mol with an MP2 correction. The Cs^+ cation sits 0.68 Å above the plane of the ether oxygens. Other changes in geometry are very small. This nonplanar configuration was also characterized by one small, imaginary harmonic frequency. The issue of numerical precision in frequency evaluation was not resolved for the $x = 3, 4$ complexes due to the expense of MP2 optimizations.

Total and incremental binding energies for the D_3 complexes are given in Tables 2 and 3, respectively. For reactants or products having imaginary frequencies, the frequencies were simply included in the enthalpy calculation as negative values. Room temperature enthalpy differences for these reactions are insensitive to the treatment of the few lowest frequencies. That is, altering them by <10 cm^{-1} would shift ΔH^{298} by less than 0.1 kcal/mol.

D. $M^+(DME)_4$. Structural parameters for the S_4 symmetry $M^+(DME)_4$ complexes are shown in Figure 6. The oxygens are located in a tetrahedral arrangement around the central cation, with C−O−C planes of DME rotated in order to minimize ligand−ligand repulsion. $Cs^+(DME)_4$ is characterized by three very small numerically unresolved frequencies (6i, 4i, and 2i). Across the $M^+(DME)_x$, $x = 1-4$, sequence of complexes, the MO bond length uniformly increases as ligands are added, due to ligand−ligand repulsion and screening of the positive charge by the other ligands.[17]

While the binding energy of the first DME varies by nearly a factor of 3 (−39.1 for Li^+ to −14.1 for Cs^+) along the sequence of alkali cations, the variation for the fourth DME is

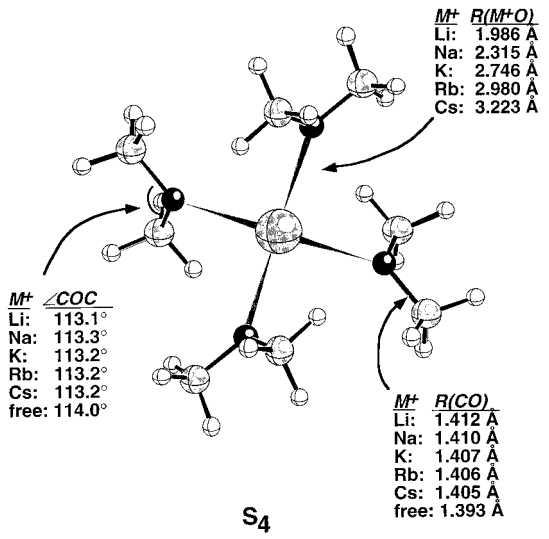

Figure 6. $M^+(DME)_4$ S_4, RHF/6-31+G* optimized structures. The Li data were taken from ref 9.

much less due to the reduced ability of the ligands to approach closer to the cation (see Table 3). Glendening and Feller studied the binding energies of multiple waters to the alkali cations[16] at the same level of theory used in the current work. They reported that the fourth water binds with nearly identical strength to the fourth DME, but only for the equivalent high-symmetry three- and four-coordinated structures. For comparison purposes, at the MP2/6-31+G* level, the $D_3 \rightarrow S_4$ fourth incremental water binding energies are −16.6 (Li^+), −14.0 (Na^+), −12.8 (K^+), −11.4 (Rb^+), and −10.2 (Cs^+) kcal/mol. The larger cations, however, prefer hydrogen-bonded water clusters and clusters that place the next water outside the first coordination sphere.

E. Trends and Comparisons. Evidence for highly electrostatic behavior is given by the partial charges on the metal and ligand atoms. A Mulliken analysis reveals a net charge range of +0.92 to +0.98*e* for Na through Cs in the various clusters. Partial charges on oxygen range from −0.63 to −0.71*e* and on the methyl groups from +0.32 to +0.38*e*. Lithium complexes, however, exhibit distinct donor-to-metal charge transfer. Li/O Mulliken charges are +0.80/−0.62*e* for Li^+-(DME) and +0.57/−0.56*e* for $Li^+(DME)_2$. A natural energy decomposition analysis[51] (NEDA) was also applied to these systems. NEDA is a useful approach for partitioning the interaction energy into electrostatic, polarization, charge transfer, and exchange repulsion components. The results are not presented here, as the qualitative trends are nearly identical with those observed for alkali metal/water clusters using the same method.[52] In summary, the electrostatic component dominates the interaction energy for each metal/ligand aggregate. Charge transfer is substantial only for the lithium complexes[9,52] and decreases rapidly with increasing cation size.

In all of the calculations discussed so far, the "(n−1)" metal shell was included in the correlation treatment for Na^+−Cs^+. The effects of choosing a different core definition in sodium are summarized in Table 5. It can be seen that incremental binding energies are underestimated by up to 1 kcal/mol with a neon-type core, and $Na^+\cdots O$ distances are overestimated by up to 0.06 Å. In fact, for these complexes the binding energies are more sensitive to the frozen core definition than to correlation recovery. Although the 6-31+G* basis set lacks sufficient flexibility for a quantitative description of core/valence effects, similar conclusions have been reached by Bauschlicher et al.[13] and by Feller et al.[15] with much larger basis sets.

TABLE 5: Effect of Using Different Na Frozen Core Definitions on the MP2 Incremental Binding Energies and Metal−Oxygen Distances in $Na^+(DME)_x$[a]

		core = [He]		core = [Ne]	
x	geom.	ΔE_i	$Na^+\cdots O$	ΔE_i	$Na^+\cdots O$
1	RHF	−26.8	2.204	−26.4	
2		−23.4	2.234	−22.9	
3		−19.3	2.271	−18.3	
4		−15.6	2.315	−14.9	
1	MP2	−26.5	2.179	−26.4	2.240
2		−23.1	2.213	−22.9	2.266

[a] CP-corrected binding energies are given in kcal/mol and distances in angstroms. All calculations were done with the 6-31+G* basis set.

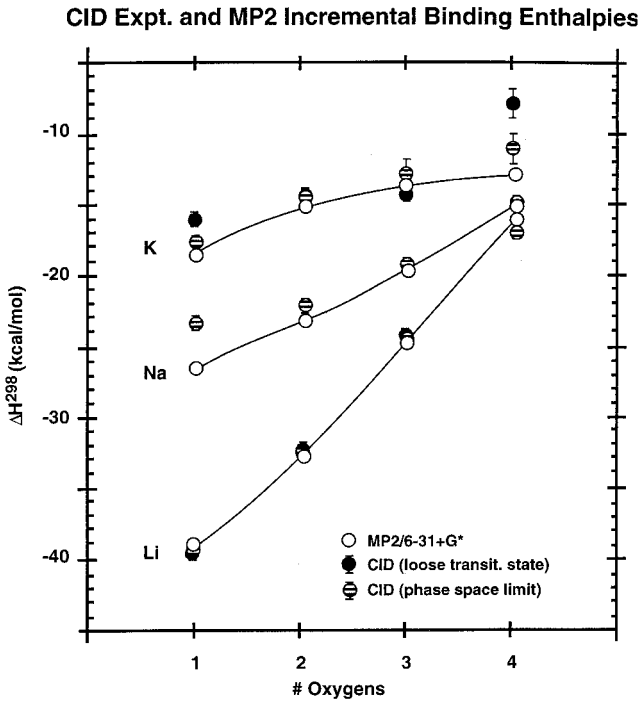

Figure 7. Comparison between collision-induced dissociation experimental binding enthalpies and MP2 results obtained with the 6-31+G* basis set.

Agreement between the MP2 incremental binding enthalpies and results obtained from collision-induced dissociation (CID) experiments[9,11] is generally excellent. Figure 7 compares the available data for Li^+, Na^+, and K^+. The primary difficulty in measuring ΔH experimentally lies in the analysis of the raw data. The apparent onset of dissociation must be corrected for the effects of multiple collisions between the cation ether complex and the rare gas atoms, variations in the internal temperature of the complex, and the unimolecular decay rate. The last of these is most problematic. Where discrepancies exist between the experimental and theoretical values, larger basis set calculations[6] have failed to resolve the issue.

IV. Summary and Conclusions

The structures and binding energies of $M^+(DME)_x$ complexes have been determined with polarized basis sets at the RHF and MP2 levels of theory. The resulting trends were discussed in terms of classical electrostatics and nonclassical behavior. Electrostatics correctly predicts (1) a monotonic decrease in total binding energies with increasing cation size accompanying the increase in $M^+\cdots O$ bond lengths with ligand coordination number, (2) a monotonic decrease in incremental binding energies, and (3) an ether dipole that is directed at the metal

ion. The incremental binding energy drops more quickly with increasing ligand coordination number for smaller cations due to relatively larger steric crowding of the ligands.

For sufficiently large polarizabilities of both ligand and metal, core polarization stabilizes bonding on the same side of the cation, promoting bending for $M^+(DME)_2$ complexes and pyramidalization for $M^+(DME)_3$ complexes. This distortion increases with cation polarizability. Quantum effects also give rise to charge transfer from the ligand to the metal in the more strongly bound clusters.[9] The computed binding enthalpies are generally in excellent agreement with the available experimental data obtained from collision-induced dissociation measurements. Where discrepancies exist, tests conducted with much larger basis sets suggest that there are further difficulties in the experimental analysis.

Acknowledgment. This research was supported by the U.S. Department of Energy under Contract No. DE-AC06-76RLO 1830. The authors acknowledge the support of the Division of Chemical Sciences, Office of Basic Energy Sciences. S.E.H. and E.D.G. also acknowledge the support of the Associated Western Universities, Inc. (on behalf of Washington State University), under Grant No. DE-FG06-89ER-75522 with the U.S. Department of Energy. The authors thank Greg Schenter for careful reading of the manuscript. We are grateful to the referee for providing clarifications to some trends involving CV contributions. Portions of this work were completed on the computer resources at the National Energy Research Supercomputer Center with a grant provided by the Scientific Computing Staff, Office of Energy Research, U.S. Department of Energy. The Pacific Northwest National Laboratory is a multiprogram national laboratory operated by Battelle Memorial Institute.

References and Notes

(1) Dang, L. X.; Kollman, P. A. *J. Am. Chem. Soc.* **1990**, *112*, 5716.
(2) Thompson, M. A.; Glendening, E. D.; Feller, D. *J. Phys. Chem.* **1994**, *98*, 10465.
(3) Glendening, E. D.; Feller, D.; Thompson, M. A. *J. Am. Chem. Soc.* **1994**, *116*, 10657.
(4) Dang, L. X. *J. Am. Chem. Soc.* **1995**, *117*, 6954.
(5) Glendening, E. D.; Feller, D. *J. Am. Chem. Soc.* **1996**, *118*, 6052.
(6) Feller, D.; Aprà, E.; Nichols, J. A.; Bernholdt, D. E. *J. Chem. Phys.* **1996**, *105*, 1940.
(7) Feller, D. Submitted to *J. Phys. Chem.*
(8) Katritzky, A. R.; Malhotra, N.; Ramanathan, R.; Kemerait, R. C., Jr.; Zimmerman, J. A.; Eyler, J. R. *Rapid Commun. Mass Spectrom.* **1992**, *6*, 25.
(9) More, M. B.; Glendening, E. D.; Ray, D.; Feller, D.; Armentrout, P. B. *J. Phys. Chem.* **1996**, *100*, 1605.
(10) Ray, D.; Feller, D.; More, M. B.; Glendening, E. D.; Armentrout, P. B. *J. Phys. Chem.* **1996**, *100*, 16116.
(11) More, M. B.; Ray, D.; Armentrout, P. B. Submitted to *J. Phys. Chem.*
(12) Clementi, E.; Popkie, H. *J. Chem. Phys.* **1972**, *57*, 1077.
(13) Bauschlicher, C. W., Jr.; Langhoff, S. R.; Partridge, H.; Rice, J. E.; Komornicki, A. *J. Chem. Phys.* **1991**, *95*, 5142.
(14) Feller, D.; Glendening, E. D.; Kendall, R. A.; Peterson, K. A. *J. Chem. Phys.* **1994**, *100*, 4981.
(15) Feller, D.; Glendening, E. D.; Woon, D. E.; Feyereisen, M. W. *J. Chem. Phys.* **1995**, *103*, 3526.
(16) Glendening, E. D.; Feller, D. *J. Phys. Chem.* **1995**, *99*, 3060.
(17) Kaupp, M.; Schleyer, P. v. R. *J. Phys. Chem.* **1992**, *96*, 7316.
(18) Bauschlicher, C. W., Jr.; Sodupe, M.; Partridge, H. *J. Chem. Phys.* **1992**, *96*, 4453.
(19) Glendening, E. D.; Feller, D. *J. Phys. Chem.* **1996**, *100*, 4790.
(20) Rosi, M.; Bauschlicher, C. W., Jr. *J. Chem. Phys.* **1990**, *92*, 1876.
(21) Bauschlicher, C. W., Jr.; Langhoff, S. R.; Partridge, H. *J. Chem. Phys.* **1991**, *94*, 2068.
(22) Magnusson, E.; Moriarty, N. W. *J. Comput. Chem.* **1993**, *14*, 961.
(23) Siegbahn, P. E. M.; Blomberg, M. R. A.; Svensson, M. *J. Phys. Chem.* **1993**, *97*, 2564.
(24) von Szentpály, L. *Chem. Phys. Lett.* **1990**, *170*, 555.
(25) Kaupp, M.; Schleyer, P. v. R.; Stoll, H.; Preuss, H. *J. Chem. Phys.* **1991**, *94*, 1360.
(26) Seijo, L.; Barandiarán, Z.; Huzinaga, S. *J. Chem. Phys.* **1991**, *94*, 3762.
(27) Rosi, M.; Bauschlicher, C. W., Jr. *Chem. Phys. Lett.* **1990**, *166*, 189.
(28) Langhoff, S. R.; Bauschlicher, C. W., Jr.; Partridge, H.; Sodupe, M. *J. Phys. Chem.* **1991**, *95*, 10677.
(29) Dzidic, I.; Kebarle, P. *J. Phys. Chem.* **1970**, *74*, 1466.
(30) Pedersen, C. J. *J. Am. Chem. Soc.* **1967**, *89*, 7017.
(31) Frensdorff, H. K. *J. Am. Chem. Soc.* **1971**, *93*, 600.
(32) Lamb, J. D.; Izatt, R. M.; Swain, C. S.; Christensen, J. J. *J. Am. Chem. Soc.* **1980**, *102*, 475.
(33) Schulz, W. W.; Bray, L. A. *Sep. Sci. Technol.* **1987**, *22*, 191.
(34) Boys, S. F.; Bernardi, F. *Mol. Phys.* **1970**, *19*, 553.
(35) Dunning, T. H., Jr. *J. Chem. Phys.* **1989**, *90*, 1007.
(36) van Duijneveldt, F. B.; van Duijneveldt-van de Rijdt, J. G. C. M.; van Lenthe, J. H. *Chem. Rev.* **1994**, *94*, 1873.
(37) Hermansson, K. *J. Chem. Phys.* **1988**, *89*, 2149.
(38) Turi, L.; Dannenberg, J. J. *J. Phys. Chem.* **1993**, *97*, 2488.
(39) Hehre, W. J.; Ditchfield, R.; Pople, J. A. *J. Chem. Phys.* **1972**, *56*, 2257.
(40) Clark, T.; Chandrasekhar, J.; Spitznagel, G. W.; Schleyer, P. v. R. *J. Comput. Chem.* **1983**, *4*, 294.
(41) Hariharan, P. C.; Pople, J. A. *Theor. Chim. Acta* **1973**, *28*, 213.
(42) Hay, P. J.; Wadt, W. R. *J. Chem. Phys.* **1985**, *82*, 299.
(43) Frisch, M. J.; Trucks, G. W.; Head-Gordon, M.; Gill, P. M. W.; Wong, M. W.; Foresman, J. B.; Johnson, B. G.; Schlegel, H. B.; Robb, M. A.; Replogle, E. S.; Gomperts, R.; Andres, J. L.; Raghavachari, K.; J. S. Binkley; Gonzalez, C.; Martin, R. L.; Fox, D. J.; Defrees, D. J.; Baker, J.; Stewart, J. J. P.; Pople, J. A. *Gaussian 92*, Revision C; Gaussian, Inc.: Pittsburgh, PA, 1992.
(44) Frisch, M. J.; Trucks, G. W.; Schlegel, H. B.; Gill, P. M. W.; Johnson, B. G.; Robb, M. A.; Cheeseman, J. R.; Keith, T.; Petersson, G. A.; Montgomery, J. A.; Raghavachari, K.; Al-Laham, M. A.; Zakrzewski, V. G.; Ortiz, J. V.; Foresman, J. B.; Cioslowski, J.; Stefanov, B. B.; Nanayakkara, A.; Challacombe, M.; Peng, C. Y.; Ayala, P. Y.; Chen, W.; Wong, M. W.; Andres, J. L.; Replogle, E. S.; Gomperts, R.; Martin, R. L.; Fox, D. J.; Binkley, J. S.; Defrees, D. J.; Baker, J.; Stewart, J. P.; Head-Gordon, M.; Gonzalez, C.; Pople, J. A. *Gaussian 94*, Revision D.1; Gaussian, Inc.: Pittsburgh, PA, 1995.
(45) Del Bene, J. E.; Mettee, H. D.; Frisch, M. J.; Luke, B. T.; Pople, J. A. *J. Phys. Chem.* **1983**, *87*, 3279.
(46) Scott, A. P.; Radom, L. *J. Phys. Chem.* **1996**, *100*, 16502.
(47) Hay, B. P.; Rustad, J. R. *J. Am. Chem. Soc.* **1994**, *116*, 6316.
(48) Hay, B. P.; Rustad, J. R.; Hostetler, C. J. *J. Am. Chem. Soc.* **1993**, *115*, 11158.
(49) Kendall, R. A.; Dunning, T. H., Jr.; Harrison, R. J. *J. Chem. Phys.* **1992**, *96*, 6796.
(50) Schäfer, A.; Horn, H.; Ahlrichs, R. *J. Chem. Phys.* **1992**, *97*, 2571.
(51) Glendening, E. D.; Streitwieser, A. *J. Chem. Phys.* **1994**, *100*, 2900.
(52) Glendening, E. D. *J. Am. Chem. Soc.* **1996**, *118*, 2473.